Quantifying the Causal Strength of Compound Drought–Heatwaves: Implications for Fire Events and Cropland Productivity

Serhan Yeşilköy

Istanbul Provincial of Agriculture and Forestry, Turkish Ministry of Agriculture and Forestry, Istanbul, Türkiye
University of Colorado, Civil, Environmental and Architectural Engineering, Boulder, CO, USA

Corresponding author: S. Yeşilköy (Serhan.Yesilkoy-1@colorado.edu)
ORCID: https://orcid.org/0000-0002-8921-6371

Abstract

Compound drought and heatwave (CDHW) events represent one of the most disruptive forms of climate extremes, as the simultaneous occurrence of dry and hot conditions signifies their impacts far beyond those of individual events. Yet, despite their increasing significance, the causal influence of CDHW frequency and severity on fire activity and crop yield variability remains poorly quantified, particularly in Mediterranean climate hotspots. This study provides a comprehensive assessment of long-term CDHW climatology across Türkiye and quantifies their causal effects on burned areas and major crop-yield anomalies through the complex causal networks based on the Peter and Clark Momentary Conditional Independence (PCMCI) framework. The findings reveal a clear intensification of CDHW conditions over recent decades, with significant upward trends in both event frequency (2.74 days/decade) and thermal severity (0.74°C/decade), particularly during winter and summer months. The causal strengths of CDHW events and severity on fire regimes explain up to 38.3% of burned-area variability and crop yield reductions during critical phenological periods, affecting both rainfed winter wheat (up to 71.6%) and irrigated crops such as maize, rice, and soybean (up to 69.8%). The spatial causal signals demonstrate that CDHW events can be considered dominant climatic stressors across Türkiye's agro-ecosystems and fire-prone landscapes. Overall, this work provides one of the first spatially explicit causal strengths of CDHW impacts on both agriculture and fire activity, indicating the importance of compound-event-aware early warning systems and climate-resilient management strategies in regions facing intensifying hot-dry extremes.

Keywords: Climate Extremes, Heat Stress, Compound Events, Causality, Ecosystem Risk.

---

1. Introduction

According to the International Disaster Database (EM-DAT) database (https://public.emdat.be/data), more than 33.1 million and 1.71 billion people have been affected, and total damage has been calculated at more than 22.7 and 261.7 billion US dollars by heatwaves and drought events around the world since 2000, respectively. The Clausius–Clapeyron equation of thermodynamics shows that for every 1°C increase in air temperature, the atmosphere can hold 6-7% additional water vapor (Allen and Ingram, 2002; Trenberth et al., 2003). The development of heatwaves results from the dynamics of Rossby waves, extensive undulations in the upper-level atmospheric jet stream. Enhanced and quasi-stationary Rossby wave patterns can contribute to extended durations of high-pressure systems persisting over an area, blocking the development of weather systems and leading to the formation of heatwaves persisting longer than three consecutive days across mid-latitudes (Domeisen et al., 2023; McGregor, 2024).

The recent ECMWF report (2026) highlighted that the past 11 years have been the 11 warmest on record. The World Meteorological Organization (WMO) (https://wmo.int/media/news/global-drought-hotspots-report-highlights-human-and-economic-impacts) also indicated that Türkiye, located in the Mediterranean Basin, is one of the most important hotspots for extreme conditions for local communities (Yeşilköy et al., 2024). Therefore, it can be said that both extreme heat or heatwaves and drought events occur simultaneously, and these events have become more common in the latest years and projected periods (Sutanto et al., 2025). These events are defined as compound drought and heatwave (CDHW) events and play a crucial role in the earth system (Romanou et al., 2024), including agricultural (Kabtih et al., 2025) and forest gross primary (Bao et al., 2025; Zhu et al., 2025) productivity.

Climate change exacerbates the frequency, duration, severity, and spatial extent of single heatwaves (Yeşilköy, 2025) and drought events on a global (Cook et al., 2020) and regional scale (Yeşilköy and Şaylan, 2022) under the latest socioeconomical scenarios (e.g., CMIP6). These events impose significant and harmful consequences on ecosystems, including agricultural and forest lands. In the literature, there are studies investigating CDHW event frequency, severity, and duration has increased in global scale (Zhang et al., 2022; Tripathy et al., 2023; Huang et al., 2025) and in different ecosystems such as croplands (Li et al., 2025; Wang et al., 2025) and their impacts on phenology (Tian et al., 2024a) in dry and humid environment (Wang et al., 2024), on forest vulnerabilities (Bastos et al., 2021), and wildfire activities (Shi et al., 2024; Zong et al., 2024) in major forests (Libonati et al., 2022), crop yield and water use efficiency reductions (Brás et al., 2021; Sutanto et al., 2024; Han et al., 2025) in breadbasket regions (Kornhuber et al., 2020; Shan et al., 2024). Sutanto et al. (2025) analyzed the compound and consecutive drought and heatwave hazard projections and found that these events are projected to show an expansion towards the southeastern part of Europe, where Türkiye is located (hotspot), based on Inter-Sectoral Impact Model Intercomparison Project (ISIMIP) model data under SSP1-2.6 and SSP5-8.5 scenarios. It can be clearly seen that CDHW events are more threatening than single drought and heatwave events. From this perspective, it is thought that a study revealing causal

relationships between CDHW events and major crop productivity and fire events will help to better understand and manage future extreme and compound events monitoring and early warning for related sectors.

The number of causal studies in climate science has been increasing to better understand the relationship among various physical processes. There are some causality algorithms inferring contemporaneous and lagged dependencies between processes. For example, Granger Causality (Granger, 1969) was the prevailing method for causal analysis that utilizes time series observations. Transfer Entropy (TE; Schreiber, 2000) is a distinct metric for quantifying the transfer of information, which is rooted in the principles of information. Cross Convergent Mapping (CCM) is a nonlinear causal inference method based on Takens' embedding theorem, which can detect linear and nonlinear causalities (Sugihara et al., 2012), which can be tested with crop yield fluctuations and drought indices (Yeşilköy et al., 2026). Runge et al. (2019) developed Peter and Clark Momentary Conditional Independence (PCMCI), which combines linear or nonlinear conditional independence tests with a causal discovery algorithm to estimate causal networks from large-scale and autocorrelated multivariate time series data. In recent years, the PCMCI causal discovery method has been successfully performed in the diverse fields of climate systems (Docquier et al., 2024), biosphere-atmosphere interactions (Krich et al., 2020), flood drivers (Miersch et al., 2025), and drought conditions and their teleconnections (Chauhan et al., 2024). In addition, Tian et al. (2024b) focused on historical changes in CHDW events and revealed the causal links with PCMCI between atmospheric drivers and CDHW events in Central Europe.

It can be seen that substantial scientific uncertainty remains on causal links between CDHW events and their regional impacts on forest and agricultural yield fluctuation. To fulfill this important scientific gap, this research is one of the first studies exploring the spatial causal relationships between CDHW events and their causal inference between crop yield reduction and fire activities. Türkiye is located in one of the most important climate change hotspots (Lazoglou et al., 2024) and has the most climate-driven susceptible forests in Europe (Forzieri et al., 2021). According to FAOSTAT, Türkiye produced 20.8 million tons of winter wheat, 180,000 tons of soybean, 1.02 million tons of rice, and 8.1 million tons of maize and ranks 10^{th}, 33^{rd}, 42^{nd}, and 19^{th} among producers in the world, respectively. Also, there has been no study conducted for the spatial causal inference between compound extreme events and agricultural productivity and fire events across Türkiye.

The purpose of this study was to answer the following research questions. (1) What is the climatology of CDHW events and their severity in Türkiye's agricultural and forest lands? (2) What are the spatial and temporal changes of CDHW events and severity? (3) Are there causal links between the number of CDHW events and severity and crop yield fluctuation and fire activities?

This paper is structured as follows: Section 2 provides a detailed description of the study area, the data source, the definition of the CDHW event and its severity, and the causal analysis

performed. The spatiotemporal characteristics of CDHW events and severity climatology and the relationship between crop yield fluctuations and burned areas between CDHW events and severity can be found in the Results (Section 3). Within Section 4, the results were compared to the other related studies and emphasize the importance of CDHW events and severity on crop yield reduction and burned areas.

2. Materials and Methods

2.1 Study Area

The study area covers the agricultural production of major field crops (e.g., winter wheat, maize, rice, and soybean) and burned areas across Türkiye (26-56°E longitude; 36-45°N latitude), located in the eastern part of the Mediterranean Basin (Figure 1) and considered a climate hotspot. Agricultural and forest lands cover 43.7 and 14.9 percent (the total percentage is calculated as 58.6%) of the total area in Türkiye based on the CORINE 2018 Land Cover dataset. Türkiye is vulnerable to extremes, including drought (Dabanlı et al., 2017) and heatwaves (Tatlı and Serkendiz et al., 2025), and it is also projected that there will be a greater number of heatwave events and longer durations (Yeşilköy, 2025) and drought conditions in the 21st century (Yavaşlı and Erlat, 2023).

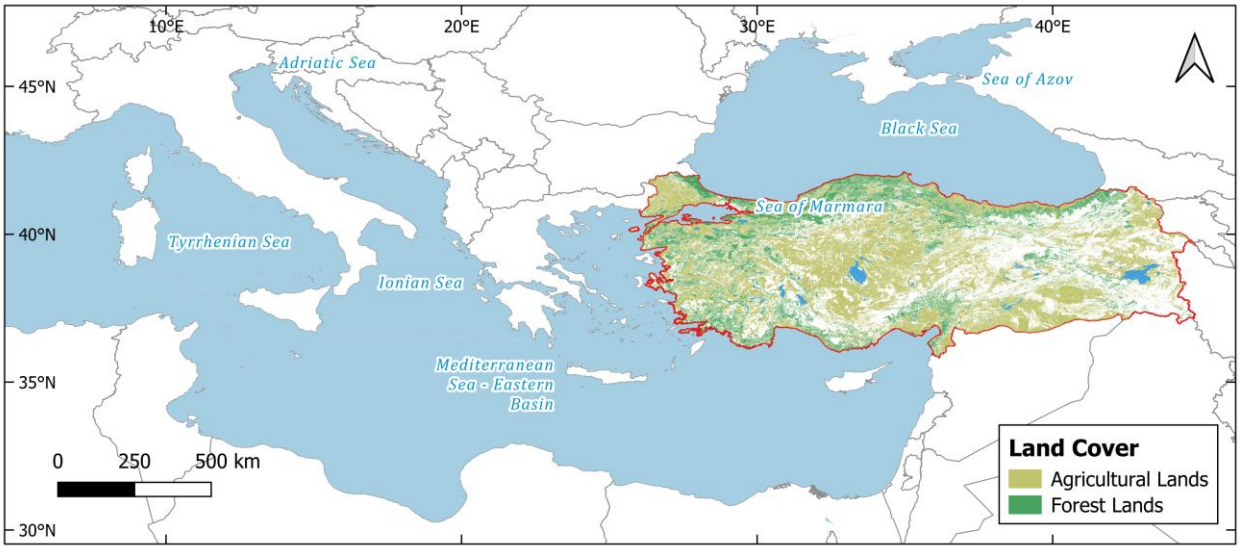

Figure 1. Yellow and green pixels represent agricultural and forest lands in Türkiye, respectively. Water bodies are represented by the blue color (CORINE, 2018). Grey and red lines are countries' and Türkiye's administrative boundaries, respectively. The vast majority of white areas in the eastern part of Türkiye are covered by mountains with significant snow water accumulation (Yeşilköy and Baydaoğlu, 2025).

2.2 Data

Gridded ERA5-land hourly reanalysis (Muñoz-Sabater et al., 2021) air temperature (°C) with 0.1-degree (~10x10 km) spatial resolution and monthly Standardized Precipitation and Evapotranspiration Index (SPEI; Vicente-Serrano et al., 2010) derived from ERA5 reanalysis (Keune et al., 2025) with 0.25-degree spatial resolution between 1965 and 2025 was downloaded from ECMWF's Copernicus Climate Data Store. This dataset shows high accuracy in a long-term period for air temperature representativeness (Yılmaz, 2023). Hourly air temperature data were converted to daily maximum temperature in each grid cell. The SPEI index is calculated based on the monthly climatic water balance deficit (precipitation and total evapotranspiration) based on the Penman-Monteith (Allen et al., 1998) approach, which is widely performed to capture drought events. SPEI at a 6-month time scale (e.g., SPEI-6) was selected to capture CDHW events and their severity (Monteiro dos Santos et al., 2024). To overlap these two datasets with different spatial resolutions, bilinear interpolation (Beguería et al., 2014), which is a reliable method for climate studies (Nouri, 2023), was performed to improve the spatial resolution of SPEI-6 data to 0.1-degree spatial resolution.

The long-term gridded with 0.25 spatial degree burned area (m^2) between 1982 and 2000 years (except 1994 due to lack of data) was developed using images acquired by the Advanced Very High-Resolution Radiometer (AVHHR) and provided by the European Space Agency (Otón et al., 2021). A dataset with the same spatial resolution from 2000 to 2019 and from 2020 to 2023 was provided by ESA-CCI based on Moderate Resolution Imaging Spectroradiometer (MODIS) and Copernicus Climate Change Service (C3S) based on Ocean and Land Colour Instrument (Sentinel-3 OLCI) sensors, respectively (Chuvieco et al., 2018). These spatiotemporal datasets were also regridded to a common 0.1-degree for the computations (Chai et al., 2026).

The global gridded historical crop yield (production per unit harvested area) for major crops (wheat, rice, soybean, and maize) from 1981 to 2016 was developed by Iizumi and Sakai (2020) with 0.5-degrees, which was regridded to 0.1-degree spatial resolution. This dataset was generated based on the countries' annual yield statistics provided by FAOSTAT and gridded using remotely-sensed leaf area index (LAI), the fraction of photosynthetically active radiation (FPAR), and reanalysis solar radiation and reported crop-specific radiation-use efficiency data (Iizumi and Sakai, 2020). The Turkish Meteorology Service (2014) published the crop phenology atlas based on valuable long-term observations from 1930 to 2012 years for Türkiye to capture the months of the most crucial phenological stages (Bakanoğulları et al., 2022) of the major field crops.

2.3 Compound Drought and Heatwave Events Characterization

A heatwave event (days) occurs when daily maximum air temperature (T_{max}) exceeds the 90th percentile-based threshold ($T_{threshold}$) for at least three consecutive days (Mukherjee and Mishra, 2021) for each grid cell, where the 90th percentile is based on a 30-year (1966-1995) long-term period (Perkins-Kirkpatrick and Gibson, 2017). This threshold was calculated based on the daily

T_{max} from the 1966-1995 period. Heatwave severity (°C) was calculated as the difference between daily T_{max} and $T_{threshold}$ (Perkins-Kirkpatrick and Lewis, 2020). A CDHW event is characterized by when both a heatwave and a drought condition occur simultaneously (Figure 2). In this study, a drought event was detected when SPEI-6 values ≤ -1, which can be considered moderate-to-extreme dry conditions. The severity of a CDHW is calculated as the difference between daily T_{max} and $T_{threshold}$ when a heatwave and a drought event occurred at the same time.

Figure 2. The graphical representation of CDHW events and their severity throughout a year.

To evaluate the long-term changes in the frequency and severity of CDHW events, a robust non-parametric statistical framework was employed. The temporal trends were quantified and tested for statistical significance through the Mann-Kendall (MK) trend test and the Theil-Sen Slope Estimator. The MK (Mann, 1945; Kendall, 1948) test is a rank-based non-parametric method that is particularly well-suited for climatological time series, as it does not require the data to follow a specific distribution and is highly resilient to the influence of outliers. A significance threshold of $p < 0.05$ was applied to identify regions with statistically robust temporal shifts. While the MK test identifies the presence and significance of a trend, the magnitude of these changes was quantified using the Theil-Sen Estimator (Sen, 1968). The results of the MK test and the Theil-Sen estimator were integrated to generate spatial maps. Grid cells exhibiting statistically significant trends ($p < 0.05$) were highlighted to identify regional hotspots of increasing CDHW risk. Areas with non-significant changes were masked or separately identified to ensure a rigorous interpretation of the climate signal.

2.4 Causality

In this study, I employed the PCMCI algorithm, a state-of-the-art causal discovery framework designed for high-dimensional time series data, addressing the challenges of high-dimensional dependencies and autocorrelation (Runge et al., 2019), to quantify the causal influence of CDHW events and their severity on crop yield reduction and burned areas of fire events. The algorithm uses a two-step process to function: PC Phase (Condition Selection): For each target variable, a collection of possible "parent" nodes (causal drivers) is found using an iterative conditional independence test (Krich et al., 2020). This step effectively reduces the dimension of the conditioning set by removing irrelevant variables. MCI Phase (Momentary Conditional Independence): Building upon the PC phase, the MCI test calculates the strength of the causal link (MCI value) by conditioning on the identified parents. This ensures that the identified relationships are not spurious correlations caused by shared drivers or auto-dependencies (Runge, 2018).

The PCMCI framework was applied with crop yield anomalies to capture contemporaneous and short-term lagged seasonal impacts, and for wildfire analysis to account for contemporaneous effects of CDHW events and their severity. The methodology is structured into three primary phases: data preprocessing and detrending, phenology-based sensitivity establishment, and gridded causal inference computations.

Annual crop yield data (1982–2016) for winter wheat, maize, rice, and soybean were first subjected to a linear detrending procedure. This step was critical to remove non-climatic signals, such as advancements in agricultural technology and management practices (Lu et al., 2017). The arithmetically indicated yields were then normalized into Z-scores to represent yield anomalies (Chen et al., 2024). Monthly burned area data (1982–2023) were utilized to represent fire activity. Unlike crop yields, burned area data were analyzed in their original temporal structure to capture the intra-annual variability of fire regimes. To ensure comparability across different climatic zones, the burned area values were log-transformed prior to causal analysis where necessary to handle the highly skewed nature of fire event distributions (Abatzoglou and Williams, 2016).

CDHW indicators were categorized into event frequency and maximum severity. For crop analysis, these were aggregated based on crops' critical phenological stages, while for wildfire analysis, monthly maximum severity and total event days were used to match the monthly fire records. For each grid cell, the PCMCI algorithm was executed independently. For wildfires, the causal link between monthly maximum CDHW severity and burned areas was tested, whereas for crops, the analysis focused on the relationship between seasonal CDHW metrics and annual yield anomalies. To ensure statistical robustness, only causal links with a significance level of $p < 0.05$ were retained (Tibau et al., 2022). The resulting MCI values were spatially illustrated to identify regional vulnerability hotspots. The PCMCI algorithm was performed thanks to the Python Tigramite package (Runge et al., 2023; https://github.com/jakobrunge/tigramite).

3. Results

Figures 2 and 3 illustrate the spatial distribution of the number of monthly CDHW events and severity across Türkiye for the last 60 years. This 60-year period was divided into two parts, 1966-1995 (the first period, P1 afterwards) and 1996-2025 (the second period, P2 afterwards), to show climatological differences.

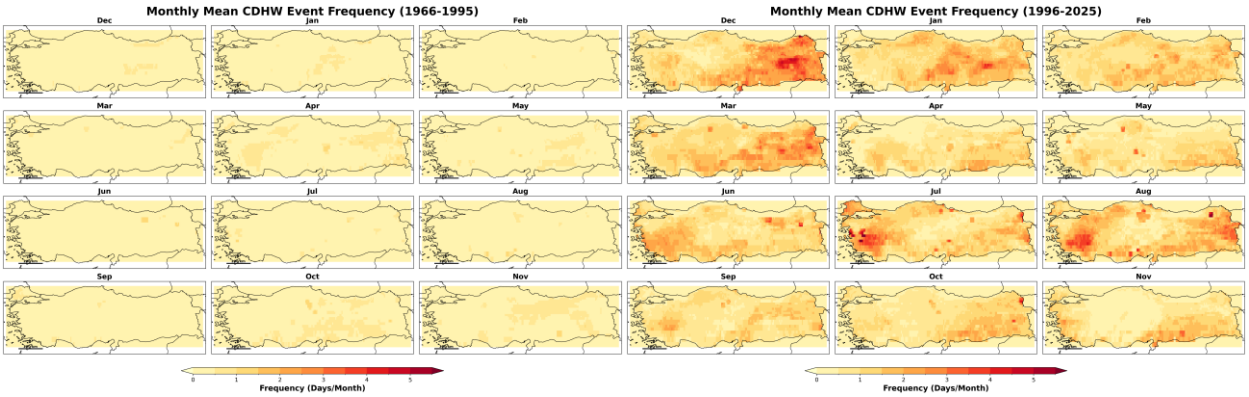

Figure 3. Spatial distribution of monthly mean CDHW event frequencies for the periods 1966–1995 (left) and 1996–2025 (right) (Reference Period: 1966-1995).

In P1, CDHW events are characterized as infrequent (0 to 1) compound events; however, in P2, the frequency of CDHW events significantly climbs throughout all months in Türkiye. The frequency increases to 4–5 days per month, especially in the summer months. A comparable scenario is observed throughout the winter season. From December to March, the frequency of CDHW events in the mountainous region is 2.9 to 3.6 days each month, with a mean value of 3.2 days. The frequency in the autumn months is changed; whereas the values were less than 1 day in the P1 period, this value is increased to a range of 2-4 days per month in most of Türkiye during the P2 period. During P1, CDHW events displayed notable localization and transience, with the mean spatial extent under compound stress consistently remaining below 0.5% for most months, reaching a minimum of 0.16% in February and a maximum of 0.74% in April. Conversely, the P2 exhibits considerable geographic expansion; for instance, the daily spatial extent in December is increased from 0.24% to 3.4%, indicating a 14-fold increase in the mean daily spatial area affected. This increase is particularly notable in August and March, with daily extents reaching peaks of 3.2% and 3.0%, respectively. The mean daily spatial extent is increased from 0.38% in P1 to 2.49% in P2.

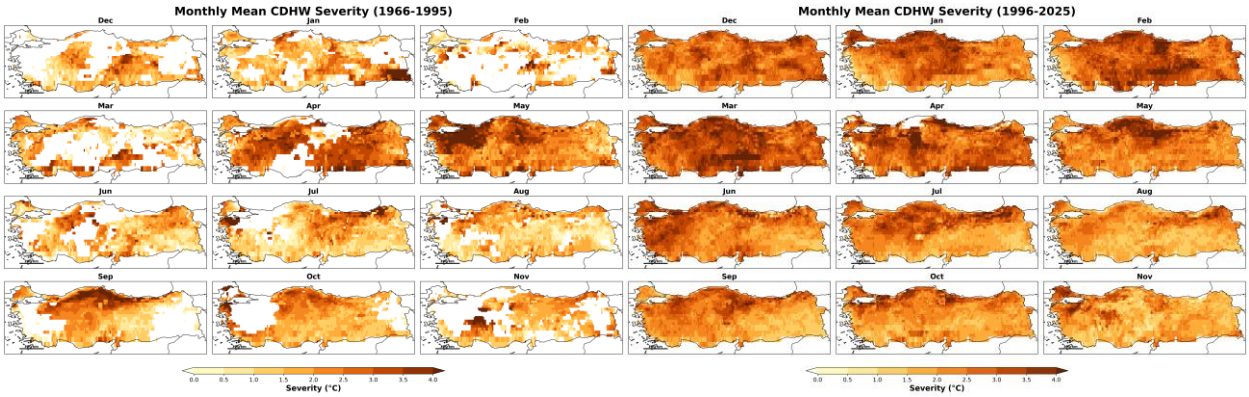

Figure 4. Spatial distribution of monthly mean CDHW severity for the periods 1966–1995 (left) and 1996–2025 (right) (Reference Period: 1966-1995).

Figure 4 illustrates a significant increase in the regional distribution of CDHW severity across all months. The intensification during the winter and early spring months (December to March) is particularly significant. In these months, mean CDHW severity is increased from 2.0 to 3.2°C. The largest increase in mean severity is calculated in March, rising from 2.1°C to 3.6°C. The mean severity increase during summer is calculated as 0.9°C from 1.7 to 2.6°C. A considerable increase in maximum CDHW severity is also detected in all months except August. Maximum CDHW severity is decreased from 10.5 to 9.6°C. Although the maximum intensity of CDHW events occurring in August during the P1 period is recorded as higher (+0.9°C), their spatial extent (ranging from 0.25 to 3.2%) and mean severity (increasing from 1.7 to 2.2°C) remained considerably more limited compared to the P2 period. During the period when spatial extent increased the most (December to March), the mean maximum severity increased from 8.2 to 13.0°C. Also, the maximum severity in March and December experienced a sharp increase from 7.8°C in P1 to 14.2°C in P2 and 7.3°C to 13.2°C, nearly doubling in intensity, respectively. The statistical analysis of changes in frequency and severity of CDHW events can be seen in Figure 5.

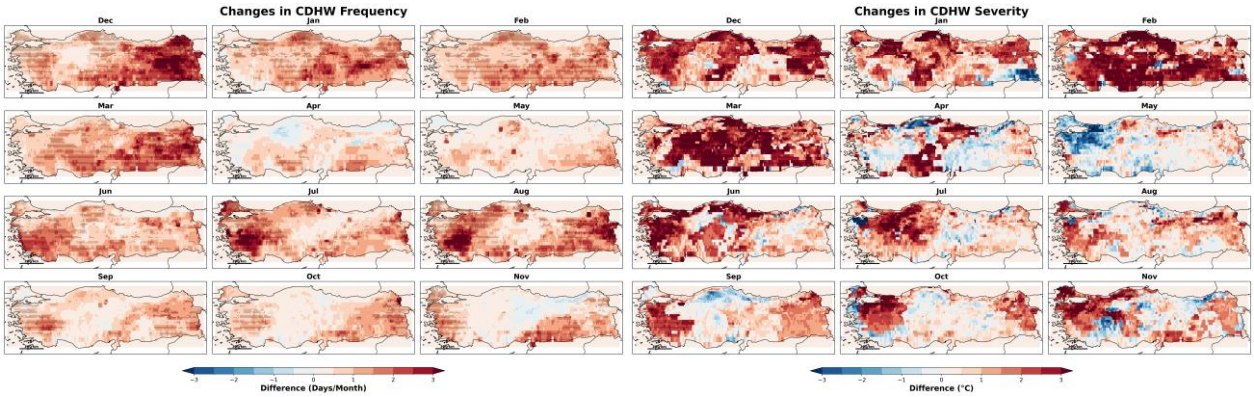

Figure 5. Changes in monthly frequency and severity of CDHW events. Black dots represent grids where the changes are significant. The trends in frequency and severity are 2.74 days/decade and 0.74°C/decade, respectively ($p<0.05$).

Figure 5 illustrates that an increase of CDHW events is not only considerable but also statistically significant across most of the regions and seasons. A large increase in both frequency and severity can be observed, with the changes being statistically significant ($p < 0.05$) during the summer months and the crucial winter-spring transition period (from December to March). From December to March, the increases in frequency (over 3.6 days/month) and severity (up to 14.2°C in maximum severity) are statistically significant across almost the entire area. Additionally, the increased frequency and severity during July and August, particularly across the Anatolian plateau (central region), indicates an intensive upward trend in compound stressors. On the other hand, frequency does not show a statistically significant decrease in any grid cell. However, some local areas show significant decreases in CDHW severity over specific months. A notable localized decrease in intensity occurs in Southeastern Anatolia in January, in the northern region in April, and in certain highly urbanized areas (the northwestern region) in May. In the end, the tendency for intensification is most clear in the western part during the autumn months. The increase in severity, which often exceeds 2°C, is statistically significant, indicating a major shift toward more severe compound extremes.

Mean burned area in hectares per year and monthly distribution can be found in Figure 6 between 1982 and 2023.

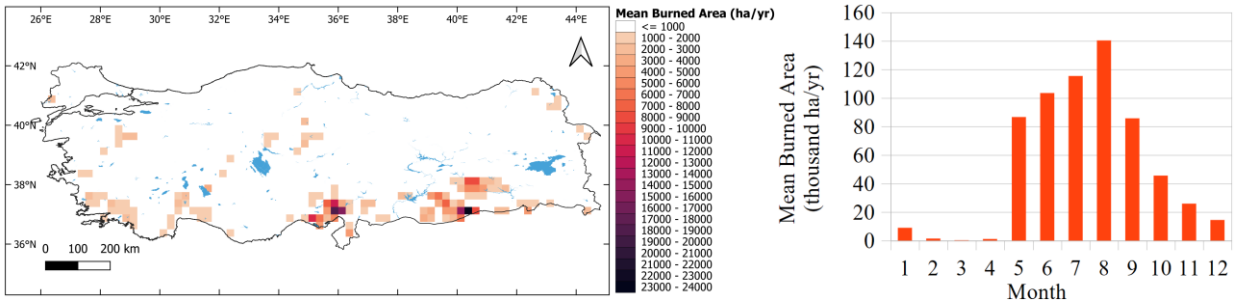

Figure 6. Fire distribution of burned area map (left) and diagram by months from 1982 to 2023 (right).

The spatial distribution of burned areas reveals a strong concentration in the southern latitudes of Türkiye, with considerable events in the western-southwestern, central, and northeastern regions. Fire affects an average of 629,500 hectares per year. The temporal distribution of fire activity is clearly seasonal, with the predominant burned area occurring from May to September; this episode covers an average of 532,000 hectares annually, constituting 84.5% of the total annual burned area. For this reason, the PCMCI was performed to provide causal links between the burned area and CDHW events and severity during these months. On the other hand, the months of October, November, December, and January represent a much smaller portion, accounting for 15.1% of the total annual burned area. Figures 7 and 8 show the spatial causal strengths and MCI values of the monthly total event and maximum severity of CDHW in the monthly total burned area, respectively.

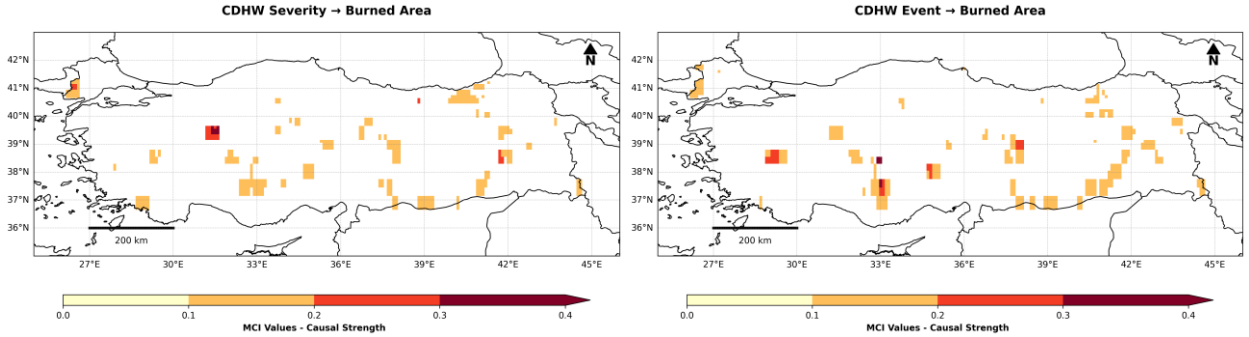

Figure 7. Causal links between burned area and (a) total CDHW events and (b) monthly maximum severity from 1981 to 2023.

Based on spatial causal analysis, the MCI values between monthly total CDHW events and monthly total burned areas range from 0.11 to 0.38, with a mean MCI value of 0.15±0.04. The MCI values correlating monthly maximum CDHW severity with monthly total burned areas range from 0.10 to 0.36, with a mean MCI value of 0.14±0.05. The spatial distribution of causal strength between the monthly total CDHW events and maximum severity, as well as the monthly total burned areas, reveals significant similarities. The maps indicate that the causal effect of CDHW events and their intensity on burned areas varies regionally, primarily focused in Central

and Southeastern regions, where hotspots for compound climate stressors related to fire dynamics are identified. The boxplots (Fig. 8) show the MCI values distribution of monthly CDHW events and their maximum severity on burned areas.

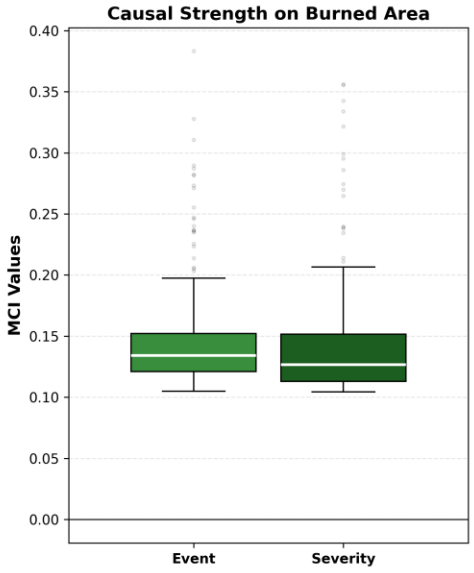

Figure 8. The MCI values distribution of burned area on total CDHW events and monthly maximum severity of selected months from 1982 to 2023.

The median MCI values are 0.134 for CDHW events and 0.126 for CDHW severity. The low interquartile range of 0.031 for events and 0.039 for severity indicates that 50% of the causal impacts are confined within these limited intervals, underscoring a high degree of consistency in this causal relationship throughout the grid cells. There are some significant outliers with MCI values of up to 0.383 for CDHW events and 0.356 for severity. This analysis shows that compound climatic stressors are the most dominant factors of the monthly total burned areas.

It can be seen from Figure 9 that the crop distribution of major crops (e.g., winter wheat, maize, rice, and soybean) covers most of Türkiye.

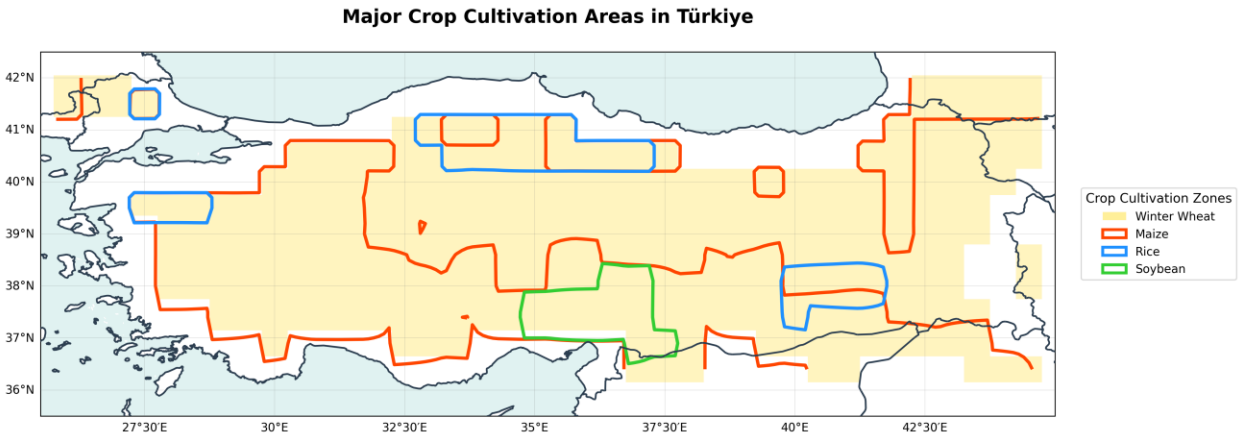

Figure 9. Crop Distribution Map from 1982 to 2016 years (Iizumi and Sakai, 2020).

Winter wheat, represented by the yellow areas, is the prevailing field crop, and 80% of winter wheat is rainfed cultivated. Most of the maize is irrigated, grown under heat stress conditions, and covers more than half of the agricultural lands (red lines). Rice is grown on around 10 percent of agricultural lands (blue parts) and cultivated under continuous flood or saturated soil conditions. Soybean cultivation is also an important legume crop in the Çukurova Region (green parts). Based on the crop phenology atlas, the critical phenological periods of the crops were determined. Winter wheat grows rapidly between April and June, and grain filling occurs during these months. Maize and soybean are vulnerable to heat stress and lack of water availability from June to August. The period from July to September is vulnerable for rice. Therefore, water availability (e.g., drought conditions) and heatwave events during these critical periods play an important role in crop productivity in Türkiye. The PCMCI calculations for each crop based on their critical phenological stages between monthly total CDHW events, maximum severity, seasonal total events, their maximum severity, and crop yield anomalies were performed. Spatial causal strength maps of the seasonal sum of total CDHW events and their maximum severity on crop yield anomalies for each crop can be found in Figures 10-13.

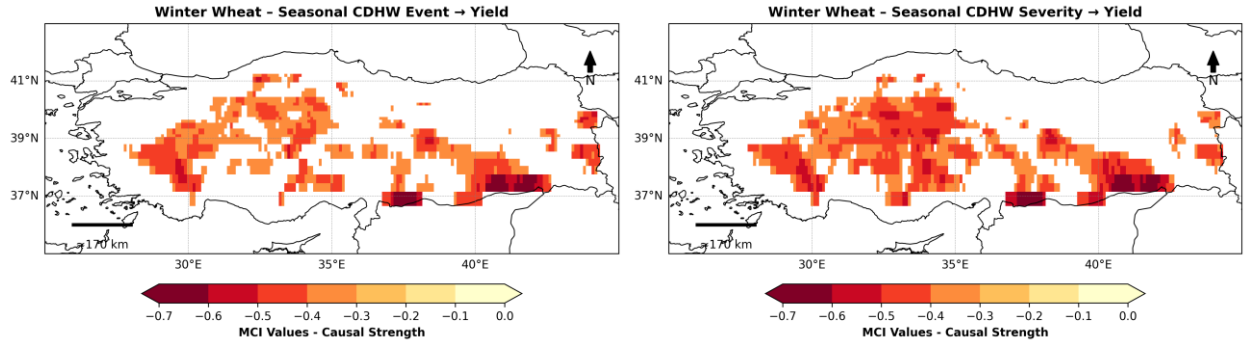

Figure 10. Spatial distribution of causal links between winter wheat yield anomalies and (left) total CDHW events and (right) monthly maximum CDHW severity during the selected phenological months from 1981 to 2016.

The spatial patterns of causal strengths reveal that winter wheat is the crop most consistently influenced by CDHW conditions across Türkiye. A substantial proportion of agricultural grid cells shows statistically significant causal links for both CDHW event frequency and severity. Mean MCI values (–0.41 for events and –0.43 for severity) indicate a strong negative influence of compound stress during the April–June phenological period, when rapid biomass accumulation and grain filling occur. The relatively narrow standard deviations (0.065–0.067) and the strong minimum values (down to –0.71 and –0.72) highlight that winter wheat experiences widespread and robust sensitivity, particularly across the Central Anatolian Plateau and Southeastern parts, which have the largest share in winter wheat production. The slightly stronger mean impact of CDHW severity compared to event count suggests that thermal excess during drought periods is a key driver of yield anomalies, aligning with the well-known vulnerability of the grain filling phase to combined heat and water stress. Overall, winter wheat demonstrates the broadest and most spatially stable causal response among all evaluated crops.

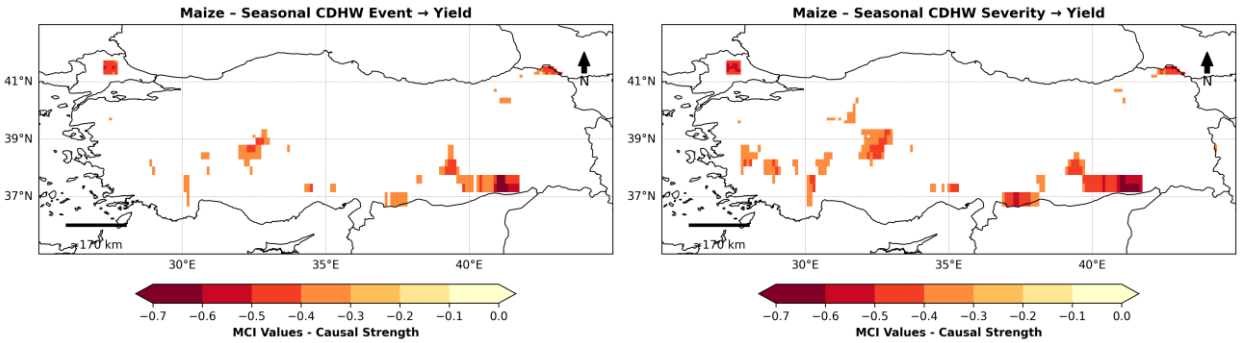

Figure 11. Spatial distribution of causal links between maize yield anomalies and (left) total CDHW events and (right) monthly maximum CDHW severity during the selected phenological months from 1981 to 2016.

The causal strength map of maize demonstrates a more limited yet distinct causal response to CDHW conditions, especially in critical production regions including the Northwestern, Western, and Southeastern areas. Nonetheless, the mean MCI values (–0.41 for events and –0.42 for severity) are comparable in magnitude to those of wheat, showing that when maize suffers, the causal relationship is strong. The minimum MCI values (ranging from –0.68 to –0.70) indicate that specific hotspots, where presumably regions with high vapor pressure deficit and severe heat stress throughout the reproductive phase from June to August, are suffering from climate stressors. The correlation between event and severity distributions indicates that maize yields are vulnerable to both CDHW events and their severity.

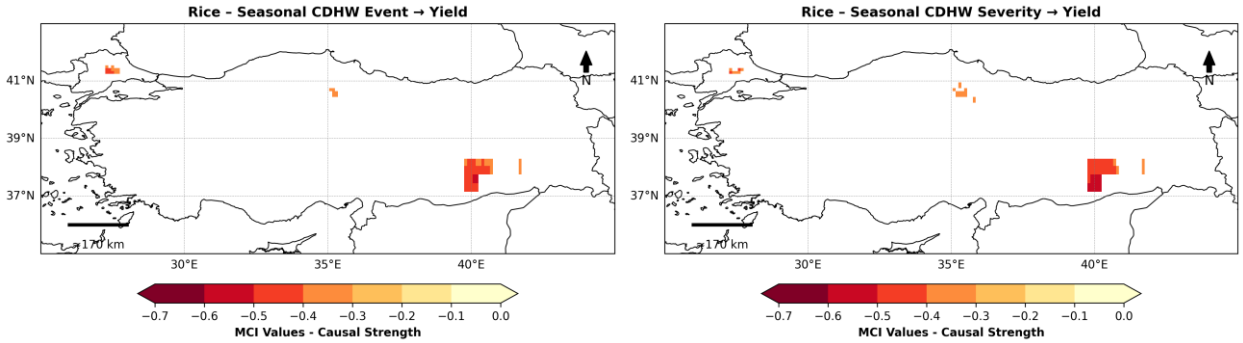

Figure 12. Spatial distribution of causal links between rice yield anomalies and (left) total CDHW events and (right) monthly maximum CDHW severity during the selected phenological months from 1981 to 2016.

For rice, there are moderate but consistent causal links to CDHW conditions in major paddy-growing areas. Significant pixels represent 13.9% of cultivated regions for both CDHW event frequency and severity. The mean MCI values (–0.41 for events and –0.44 for severity) suggest a strong causal influence. Minimum values (–0.54 to –0.59) imply that while rice production systems benefit from controlled flooding, high-temperature anomalies during the July–September window still cause considerable yield loss, particularly through impacts on panicle initiation and grain sterility. The slightly stronger influence of CDHW severity compared to event count indicates that rice is more affected by the intensity of hot-dry episodes rather than their recurrence.

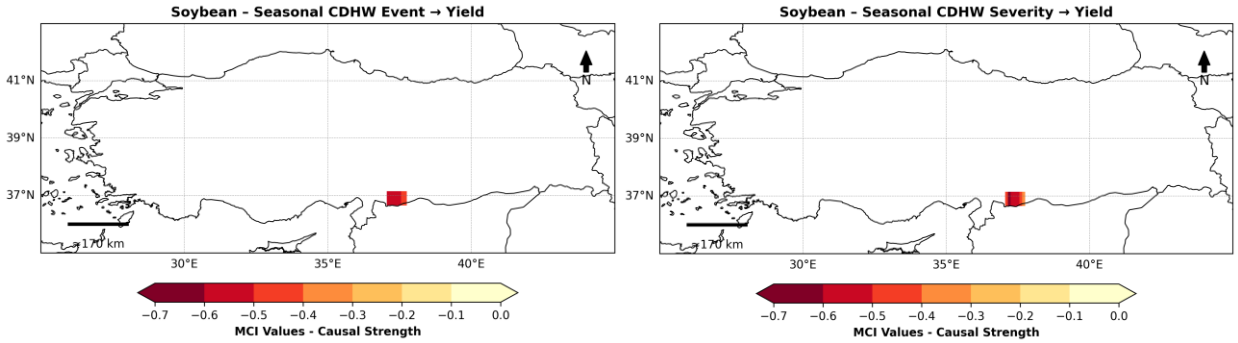

Figure 13. Spatial distribution of causal links between soybean yield anomalies and (left) total CDHW events and (right) monthly maximum CDHW severity during the selected phenological months from 1981 to 2016.

Soybean demonstrates the most spatially limited but also the strongest mean causal response to CDHW stress among all crops. Only 6.4% of soybean-growing pixels show significant causal links, reflecting its confined cultivation zone in the Çukurova region. The mean MCI values (–0.53 for events and –0.51 for severity) are the most negative among all crops, reflecting that soybean cultivation experiences a disproportionately serious effect on yield loss due to CDHW occurrences. Minimum MCI values (–0.60 to –0.62) show significant sensitivity during the reproductive phase from June to August, characterized by high water requirements and heat sensitivity. Soybean has a nearly equivalent impact from event frequency and severity, indicating that both the events and intensity of hot-dry conditions affect physiological processes throughout the flowering and pod-setting stages.

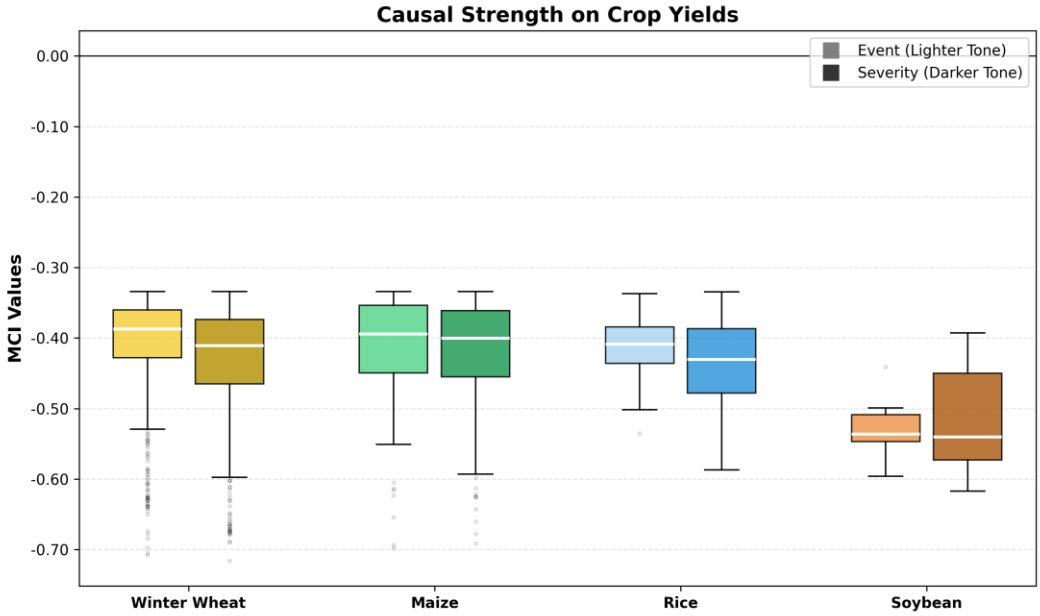

Figure 14. Distribution of MCI values showing the causal influence of total CDHW events and monthly maximum CDHW severity on yield anomalies of major crops during crop-specific critical phenological periods (1981–2016).

The boxplot analysis of the causal strengths reveals clear and crop-specific sensitivities for yield anomalies to CDHW conditions across Türkiye. Winter wheat exhibits the broadest and most homogeneous response, with relatively narrow interquartile ranges for both CDHW event frequency (IQR = 0.07) and severity (IQR = 0.09), and median MCI values clustering near -0.39 and -0.41, respectively. The lower whiskers extending to -0.53 for events and -0.60 for severity indicate that a substantial portion of wheat-growing regions experiences pronounced negative causal impacts. Maize displays a comparable but slightly more dispersed response, with wider IQRs (0.10 for events; 0.09 for severity) and similarly negative medians around –0.39 to –0.40. The deeper minimum values (-0.70 to -0.69) highlight the existence of strong, spatially concentrated hotspots where CDHW conditions exert disproportionately large influences on reproductive-stage yield outcomes. Rice demonstrates a more moderate pattern, reflected in the tight IQR for event-based causality (0.05) but stronger tail sensitivity for severity (minimum = -0.59), suggesting that while CDHW events affect rice uniformly, extreme heat intensity during flooded growing conditions remains a dominant driver of stress-induced yield reductions. Soybean stands out with the strongest median causal effects among all crops (-0.54 for events; -0.54 for severity), despite having the smallest spatial portion. Boxplots of soybean MCI values are shifted uniformly toward more negative values, and the severity metric shows the widest dispersion (IQR=0.12) and the deepest minimum (-0.62), showing soybean's vulnerability to CDHW conditions during flowering and setting pod periods. Collectively, these distributions

demonstrate that all crops experience significant causal impacts from CDHW events and their magnitude.

4. Discussion

This study investigated the spatiotemporal impact of CDHW occurrences on fire activity and agricultural productivity throughout Türkiye, considered a climate-change hotspot where extensive croplands and forests are increasingly susceptible to extreme climatic stressors. Utilizing the PCMCI causal discovery framework on long-term gridded datasets of climate, burned area, and crop yield, while considering crop-specific critical phenological periods, I assessed whether the frequency and thermal severity of CDHW events have statistically significant causal impacts. The investigation utilized high-resolution reanalysis data, long-term gridded crop yields to identify sensitivity in major crop yields, and burned areas to elucidate the causal mechanisms by which CDHW extremes influence fire dynamics and crop yield anomalies. Figures 3-5 demonstrated marked increases in both the frequency and the severity of CDHW occurrences when comparing the 1996–2025 to the 1966–1995 periods, with statistically significant trends ($p<0.05$) across the country. Strong intensification from December to March and during summer months suggests an elongation of the hot–dry season and a widening of the thermal envelope within which agriculture, ecosystems, and fire regimes operate. This shift in CDHW occurrences—more days meeting concurrent hot and dry thresholds and higher temperature exceedances—creates the preconditions for enhanced climate-impact synchrony on crops and fires detected by our causal analysis. These findings are consistent with broader assessments that show a positive trend in CDHW frequency and severity globally (Wang et al., 2025) and across the Mediterranean Basin (Petrou and Kassomenos, 2025), highlighting the growing relevance of CDHW dynamics for regional impact assessments.

Fire activity in Türkiye is seasonal (May–September) and geographically concentrated toward southern and western parts (Fig. 6). The MCI maps show significant causal links between monthly burned area and both (i) total monthly CDHW events and (ii) monthly maximum CDHW severity, with spatial hotspots over Central and Southeastern regions (Fig. 7). The distributions of MCI values indicate comparable mean causal strengths for events (range is from 0.11 to 0.38) and severity (range is from 0.10 to 0.36), alongside notable outliers that mark locations where CDHW events become important factors on burned area variability (Fig. 10). These findings show that CDHW events elevate fuel aridity and flammability, while extreme heat peaks accelerate fuel curing and reduce live-fuel moisture, enabling larger or more frequent burns even under similar conditions. Such findings align with the general conclusion that CDHW events increase the risk of wildfire globally (AghaKouchak et al., 2020; Messori et al., 2025) and in eastern-southern Europe (Santos et al., 2024).

The major crops (Fig. 9), such as winter wheat, are grown in large areas and under mostly rainfed conditions. (Keser et al., 2018). Other crops like maize and soybean are grown primarily irrigated (Bakal et al., 2017), and rice is grown under flooded or saturated conditions (Çebi et al., 2023). Even though irrigation creates contrasting hydrologic buffers against CDHW events, it

does not negate thermal stress, and phenology-based aggregation of CDHW metrics ensures that the causal analysis targets sensitive periods (e.g., April–June for wheat; June–August for maize/soybean; July–September for rice). These systemic and phenological contrasts help explain the heterogeneous MCI distributions across crops that follow. Fig. 10 reveals the broadest and most spatially significant causal response for winter wheat, particularly across the semi-arid Central Anatolian Plateau, with significant mean MCI values for both CDHW frequency (–0.41) and severity (–0.43). The slightly stronger impact of severity relative to event count indicates that thermal excess during CDHW periods is a principal driver of yield reductions, consistent with the vulnerability of grain filling to combined extreme heat and lack of soil water content in the April–June period, implying widespread and coherent sensitivity under rainfed production. He et al. (2022) selected three cases in 2003 France, 2010 Russia, and 2018 Germany to investigate the effects of CDHW events on winter wheat yield reduction. The mean crop yield reduction of three cases was 20%. The MCI values of this study represent the stronger causal strengths of CDHW events their severity in the reduction of winter wheat yields in Türkiye. Maize exhibits localized yet strong causal links in many regions of Türkiye (Fig. 11). While irrigation mitigates the effects of drought, maize still shows clear sensitivity to CDHW events and their severity. The lower-tail extremes in the boxplots (–0.69 to –0.70) and clusters in most parts suggest that extreme heat during silking and early grain fill periods cannot be fully compensated by water supply, yielding pronounced negative anomalies where vapor pressure deficit (VPD) and canopy temperature increase. Simanjuntak et al. (2023) focused on the causal impacts of heatwaves and drought events on maize yield using PCMCI in South Africa between 1986 and 2016. Their results in the northwestern part of South Africa showed that maize yields have slightly more causal strength (46%) to CDHW events compared to all parts of Türkiye (41%). Despite a smaller spatial extent (Fig. 12), rice yield reduction shows consistent causal effects, especially for CDHW severity (44%), which exhibits stronger tails than event frequency (41%). This asymmetry implies that thermal intensity, rather than the mere number of CDHW events, is the more critical factor under flooded conditions. The interpretation aligns with rice's physiological sensitivity to nighttime heat and extreme daytime temperatures, which can elevate spikelet sterility and reduce grain filling even when water is abundant (Fleisher et al., 2022). Fu et al. (2023) quantified the impacts of heatwaves and drought events on rice yield reduction between 1999 and 2012 across China and calculated their effects as $5.4 \pm 1.7\%$ and $4.2 \pm 1.1\%$, respectively. Hassan et al. (2026) showed that dry-hot events statistically significantly reduced the yields of maize and winter wheat crops in Europe during the period 1979-2021. Soybean shows the most negative median MCI (Fig. 14) among the crops, despite its limited cultivated area (Fig. 9), and severity exhibits the widest dispersion. Together with the significant lower tails, these patterns indicate high susceptibility to CDHW events (-51%) and their severity (-53%) during flowering and pod set when irrigation cannot fully buffer canopy-level thermal stress (Fig. 13). Lesk et al. (2022) reviewed the impacts of compound events on global crop yields and highlighted that the US Midwest experienced significant soybean yield loss linked to the drought and heat events in 2012.

Although CDHW events exhibited clear and statistically significant causal impacts, the causal strengths for burned areas were generally lower than crop-yield reductions. This is expected because wildfire behavior is influenced by several additional key drivers such as high wind speed (Dong et al., 2021), snow drought conditions of the previous winter (Westerling et al., 2006), and high VPD (Rao et al., 2022), which interact with, but also operate independently from, hot–dry extremes. As a result, CDHW metrics alone cannot fully capture the multi-factor nature of fire dynamics, whereas crop responses are more directly tied to compound hot–dry stress during critical phenological stages.

While regridding SPEI-6, burned areas, and crop yield data to a 0.1-degree spatial resolution using bilinear interpolation, along with phenology-based aggregation, enables spatially consistent inference, it is highly likely that more areas will be locally affected. Based on the findings of our study, some specific recommendations can be made to enhance the management strategies of agricultural and forest lands.

- Early warning systems: The findings emphasize the significance of early warning systems that monitor not only CDHW occurrences but also other climatic stressors, offering prompt advice for agricultural management and fire response preparation.
- Climate-Resilient Infrastructure: The significant causal effects observed in both rainfed and irrigated systems underscore the necessity for climate-resilient agricultural and landscape infrastructure, including efficient irrigation networks and innovative practices such as agrivoltaics, to mitigate vulnerability to climate-driven hazards.
- Integration of Climate Risk into Planning: Incorporating CDHW-based risk metrics into agricultural scheduling, crop selection, and forest management strategies is crucial for enhancing long-term resilience, as both the frequency and severity of CDHW events were identified as important factors influencing crop yield anomalies and fire activity.

5. Conclusion

The primary objective of this study was to (i) reveal the climatology of CDHW events and (ii) determine whether the frequency and severity of CDHW events have statistically significant causal influences on fire activity and crop yield reductions across Türkiye, a climate hotspot, where extensive agricultural and forest areas are increasingly exposed to extreme hot–dry conditions. Using long-term gridded climate, burned-area, crop yield datasets, and crop-specific phenological periods, the PCMCI causal discovery framework was employed to quantify causal strengths.

The results reveal that both CDHW frequency and thermal severity have significant causal strengths on burned-area dynamics, with particularly strong effects in Central and Southeastern regions where compound conditions are recurrent and fuel aridity responds rapidly to synchronous hot-dry extremes. Similarly, CDHW metrics also have crop-specific causal effects on yield anomalies: winter wheat, predominantly rainfed, shows the broadest and most spatially consistent sensitivity; irrigated maize and soybean remain highly vulnerable to CDHW event and severity despite supplemental water; and rice experiences strong yield impacts from extreme

thermal peaks even under flooded conditions. These outcomes demonstrate that both the recurrence and intensity of CDHW events shape agricultural and ecological outcomes during critical phenological and seasonal periods.

The study emphasizes the necessity of incorporating awareness of CDHW events into agricultural planning, wildfire preparedness, and climate impact assessment. By highlighting where and when CDHW events most strongly influence production and fire risk, the findings provide a data-driven foundation for improving early-warning capabilities, informing resource allocation, and supporting adaptive management in vulnerable sectors. Ultimately, the results emphasize the urgent need to adopt compound-event monitoring frameworks, enhance climate-resilient agricultural and landscape infrastructure, and develop long-term adaptation strategies tailored to the increasing likelihood of extreme hot-dry conditions across Türkiye.

Credit Authorship Contribution Statement

Serhan Yeşilköy: Conceptualization; Methodology; Data Collection and Processing; Analysis; Writing – Original Draft.

Declaration of Competing Interest

The author declares that I have no known competing financial interests or personal relationships that could have appeared to influence the work reported in this paper.

Data Availability

All data used in this study are publicly available. CORINE 2018 map can be found at https://doi.org/10.2909/960998c1-1870-4e82-8051-6485205ebbac (Last accessed on 20.02.2026). ERA5-land hourly reanalysis data can be download from https://doi.org/10.24381/cds.e2161bac (Last accessed on 20.02.2026). Monthly SPEI-6 data can be found at https://doi.org/10.24381/9bea5e16. Gridded crop yield data from 1981 to 2016 can be found at https://doi.org/10.1594/PANGAEA.909132 (Last accessed on 20.02.2026). ESA and ECMWF provide gridded burned area data (between 1982 and 2023 years) can be obtained from https://geogra.uah.es/fire_cci/fireccilt11.php and https://doi.org/10.24381/cds.f333cf85, respectively (Last accessed on 20.02.2026). All gridded data were regridded to 0.1-degree to provide spatial resolution consistency. Crop phenological atlas were provided by Turkish Meteorology Service through https://www.mgm.gov.tr/FILES/genel/kitaplar/Fenoloji_atlasi.pdf (In Turkish, last accessed on 20.02.2026).

References

Abatzoglou, J. T., & Williams, A. P. (2016). Impact of anthropogenic climate change on wildfire across western US forests. *Proceedings of the National Academy of sciences*, *113*(42), 11770-11775. https://doi.org/10.1073/pnas.1607171113

AghaKouchak, A., Chiang, F., Huning, L. S., Love, C. A., Mallakpour, I., Mazdiyasni, O., ... & Sadegh, M. (2020). Climate extremes and compound hazards in a warming world. *Annual review of earth and planetary sciences*, *48*(1), 519-548. https://doi.org/10.1146/annurev-earth-071719-055228

Allen, R. G., Pereira, L. S., Raes, D., & Smith, M. (1998). FAO Irrigation and drainage paper No. 56. *Rome: food and agriculture organization of the United Nations*, *56*(97), e156. https://www.fao.org/4/X0490E/X0490E00.htm

Allen, M. R., & Ingram, W. J. (2002). Constraints on future changes in climate and the hydrologic cycle. *Nature*, *419*(6903), 224-232. https://doi.org/10.1038/nature01092

Bakal, H., Gulluoglu, L., Onat, B., & Arıoglu, H. (2017). The effect of growing seasons on some agronomic and quality characteristics of soybean varieties in Mediterranean Region in Turkey. *Turkish Journal of Field Crops*, *22*(2), 187-196. https://doi.org/10.17557/tjfc.356213

Bastos, A., Orth, R., Reichstein, M., Ciais, P., Viovy, N., Zaehle, S., ... & Sitch, S. (2021). Vulnerability of European ecosystems to two compound dry and hot summers in 2018 and 2019. *Earth system dynamics*, *12*(4), 1015-1035. https://doi.org/10.5194/esd-12-1015-2021

Beguería, S., Vicente-Serrano, S. M., Reig, F., & Latorre, B. (2014). Standardized precipitation evapotranspiration index (SPEI) revisited: parameter fitting, evapotranspiration models, tools, datasets and drought monitoring. *International journal of climatology*, *34*(10), 3001-3023. https://doi.org/10.1002/joc.3887

Bakanoğulları, F., Şaylan, L., & Yeşilköy, S. (2022). Effects of phenological stages, growth and meteorological factor on the albedo of different crop cultivars. *Italian Journal of Agrometeorology*, *1*, 23-40. https://doi.org/10.1016/10.36253/ijam-1445

Brás, T. A., Seixas, J., Carvalhais, N., & Jägermeyr, J. (2021). Severity of drought and heatwave crop losses tripled over the last five decades in Europe. *Environmental Research Letters*, *16*(6), 065012. https://doi.org/10.1088/1748-9326/abf004

Chai, Y., Miao, C., AghaKouchak, A., Pokhrel, Y., Fu, Y., Li, X., ... & Peñuelas, J. (2026). Flash droughts exacerbate global vegetation loss and delay recovery. *Nature Communications, 17*, 485. https://doi.org/10.1038/s41467-025-67173-x

Chauhan, T., Chandel, V., & Ghosh, S. (2024). Global land drought hubs confounded by teleconnection hotspots in equatorial oceans. *npj Climate and Atmospheric Science*, *7*(1), 15. https://doi.org/10.1038/s41612-023-00558-1

Chen, X., Wang, L., Cao, Q., Sun, J., Niu, Z., Yang, L., & Jiang, W. (2024). Response of global agricultural productivity anomalies to drought stress in irrigated and rainfed agriculture. *Science China Earth Sciences*, *67*(11), 3579-3593. https://doi.org/10.1007/s11430-023-1328-2

Chuvieco, E., Lizundia-Loiola, J., Pettinari, M. L., Ramo, R., Padilla, M., Tansey, K., ... & Plummer, S. (2018). Generation and analysis of a new global burned area product based on

MODIS 250 m reflectance bands and thermal anomalies. *Earth System Science Data*, *10*(4), 2015-2031. https://doi.org/10.5194/essd-10-2015-2018

Cook, B. I., Mankin, J. S., Marvel, K., Williams, A. P., Smerdon, J. E., & Anchukaitis, K. J. (2020). Twenty-first century drought projections in the CMIP6 forcing scenarios. *Earth's Future*, *8*(6), e2019EF001461. https://doi.org/10.1029/2019EF001461

Çebi, U., Özer, S., Öztürk, O., Aydın, B., & Çakır, R. (2023). Yield and water productivity of rice grown under different irrigation methods. *The Journal of Agricultural Science*, *161*(3), 387-397. https://doi.org/10.1017/S0021859623000308

Dabanlı, İ., Mishra, A. K., & Şen, Z. (2017). Long-term spatio-temporal drought variability in Turkey. *Journal of Hydrology*, *552*, 779-792. https://doi.org/10.1016/j.jhydrol.2017.07.038

Docquier, D., Di Capua, G., Donner, R. V., Pires, C. A., Simon, A., & Vannitsem, S. (2024). A comparison of two causal methods in the context of climate analyses. *Nonlinear Processes in Geophysics*, *31*(1), 115-136. https://doi.org/10.5194/npg-31-115-2024

Domeisen, D. I., Eltahir, E. A., Fischer, E. M., Knutti, R., Perkins-Kirkpatrick, S. E., Schär, C., ... & Wernli, H. (2023). Prediction and projection of heatwaves. *Nature Reviews Earth & Environment*, *4*(1), 36-50. https://doi.org/10.1038/s43017-022-00371-z

Dong, L., Leung, L. R., Qian, Y., Zou, Y., Song, F., & Chen, X. (2021). Meteorological environments associated with California wildfires and their potential roles in wildfire changes during 1984–2017. *Journal of Geophysical Research: Atmospheres*, *126*(5), e2020JD033180. https://doi.org/10.1029/2020JD033180

EM-DAT Database (2026) https://public.emdat.be/ (Last Accessed on 20.02.2026)

Fleisher, D. H., Barnaby, J. Y., Li, S., & Timlin, D. (2022). Response of a US rice hybrid variety to high heat at Two CO2 concentrations during anthesis and grainfill. *Agricultural and Forest Meteorology*, *323*, 109058. https://doi.org/10.1016/j.agrformet.2022.109058

Forzieri, G., Girardello, M., Ceccherini, G., Spinoni, J., Feyen, L., Hartmann, H., ... & Cescatti, A. (2021). Emergent vulnerability to climate-driven disturbances in European forests. *Nature communications*, *12*(1), 1081. https://doi.org/10.1038/s41467-021-21399-7

Fu, J., Jian, Y., Wang, X., Li, L., Ciais, P., Zscheischler, J., ... & Zhou, F. (2023). Extreme rainfall reduces one-twelfth of China's rice yield over the last two decades. *Nature Food*, *4*(5), 416-426. https://doi.org/10.1038/s43016-023-00753-6

Granger, C. W. (1969). Investigating causal relations by econometric models and cross-spectral methods. *Econometrica: journal of the Econometric Society*, 424-438. https://doi.org/10.2307/1912791

Hassan, W. U., Nayak, M. A., Saharwardi, M. S., Gandham, H., Dasari, H. P., Ammann, C., ... & Abualnaja, Y. (2026). The growing threat of spatially synchronized dry-hot events to global ecosystem productivity. *Communications Earth & Environment, 7,* 178. https://doi.org/10.1038/s43247-026-03203-w

He, Y., Fang, J., Xu, W., & Shi, P. (2022). Substantial increase of compound droughts and heatwaves in wheat growing seasons worldwide. *International Journal of Climatology*, *42*(10), 5038-5054. https://doi.org/10.1002/joc.7518

Huang, S., Wang, S., Wang, C., Zhang, X., Gong, J., & Chen, N. (2025). Differential sensitivities of three types of compound drought and heatwave events to human-induced climate change across the globe. *Weather and Climate Extremes*, 100836. https://doi.org/10.1016/j.wace.2025.100836

Iizumi, T., & Sakai, T. (2020). The global dataset of historical yields for major crops 1981–2016. *Scientific Data*, *7*(1), 97. https://doi.org/10.1038/s41597-020-0433-7

The ECMWF (2026) https://www.ecmwf.int/en/about/media-centre/news/2025/2025-third-warmest-year (Last Accessed on 20.02.2026)

Kabtih, A. K., & Qian, C. (2025). Risk of successive hot-pluvial extremes on crop yield loss over global breadbasket regions. *Communications Earth & Environment, 6,* 1040. https://doi.org/10.1038/s43247-025-02989-5

Kendall, M. G. (1975). *Rank Correlation Methods*. Griffin, London.

Keser, M., Gummadov, N., Akin, B., Belen, S., Mert, Z., Taner, S., ... & Ozdemir, F. (2017). Genetic gains in wheat in Turkey: Winter wheat for dryland conditions. *The Crop Journal*, *5*(6), 533-540. https://doi.org/10.1016/j.cj.2017.04.004

Keune, J., Di Giuseppe, F., Barnard, C., Damasio da Costa, E., & Wetterhall, F. (2025). ERA5–Drought: Global drought indices based on ECMWF reanalysis. *Scientific Data*, *12*(1), 616. https://doi.org/10.1038/s41597-025-04896-y

Kornhuber, K., Coumou, D., Vogel, E., Lesk, C., Donges, J. F., Lehmann, J., & Horton, R. M. (2020). Amplified Rossby waves enhance risk of concurrent heatwaves in major breadbasket regions. *Nature Climate Change*, *10*(1), 48-53. https://doi.org/10.1038/s41558-019-0637-z

Krich, C., Runge, J., Miralles, D. G., Migliavacca, M., Perez-Priego, O., El-Madany, T., ... & Mahecha, M. D. (2020). Estimating causal networks in biosphere–atmosphere interaction with the PCMCI approach. *Biogeosciences*, *17*(4), 1033-1061. https://doi.org/10.5194/bg-17-1033-2020

Lazoglou, G., Papadopoulos-Zachos, A., Georgiades, P., Zittis, G., Velikou, K., Manios, E. M., & Anagnostopoulou, C. (2024). Identification of climate change hotspots in the Mediterranean. *Scientific reports*, *14*(1), 29817. https://doi.org/10.1038/s41598-024-80139-1

Lesk, C., Anderson, W., Rigden, A., Coast, O., Jägermeyr, J., McDermid, S., ... & Konar, M. (2022). Compound heat and moisture extreme impacts on global crop yields under climate change. *Nature Reviews Earth & Environment*, *3*(12), 872-889. https://doi.org/10.1038/s43017-022-00368-8

Libonati, R., Geirinhas, J. L., Silva, P. S., Russo, A., Rodrigues, J. A., Belém, L. B., ... & Trigo, R. M. (2022). Assessing the role of compound drought and heatwave events on

unprecedented 2020 wildfires in the Pantanal. *Environmental Research Letters*, *17*(1), 015005. https://doi.org/10.1088/1748-9326/ac462e

Li, Y., Zeleke, K., Wang, B., & Liu, D. L. (2025). A review of data for compound drought and heatwave stress impacts on crops: Current progress, knowledge gaps, and future pathways. *Plants*, *14*(14), 2158. https://doi.org/10.3390/plants14142158

Lu, W., Atkinson, D. E., & Newlands, N. K. (2017). ENSO climate risk: predicting crop yield variability and coherence using cluster-based PCA. *Modeling Earth Systems and Environment*, *3*(4), 1343-1359. https://doi.org/10.1007/s40808-017-0382-0

Mann, H. B. (1945). Nonparametric tests against trend. *Econometrica: Journal of the econometric society*, 245-259. https://doi.org/10.2307/1907187

McGregor, G. (2024). Synoptic Scale Atmospheric Processes and Heatwaves. In *Heatwaves: Causes, Consequences and Responses.* Biometeorology, vol 6. Springer, Cham. https://doi.org/10.1007/978-3-031-69906-1_6

Messori, G., Muheki, D., Batibeniz, F., Bevacqua, E., Suarez-Gutierrez, L., & Thiery, W. (2025). Global mapping of concurrent hazards and impacts associated with climate extremes under climate change. *Earth's Future*, *13*(6), e2025EF006325. https://doi.org/10.1029/2025EF006325

Miersch, P., Günther, W., Runge, J., & Zscheischler, J. (2025). Evaluating the Robustness of PCMCI+ for Causal Discovery of Flood Drivers. *Artificial Intelligence for the Earth Systems*, *4*(4), 240114. https://doi.org/10.1175/AIES-D-24-0114.1

Monteiro dos Santos, D., de Oliveira, A. M., Duarte, E. S., Rodrigues, J. A., Menezes, L. S., Albuquerque, R., ... & Libonati, R. (2024). Compound dry-hot-fire events connecting Central and Southeastern South America: an unapparent and deadly ripple effect. *npj Natural Hazards*, *1*(1), 32. https://doi.org/10.1038/s44304-024-00031-w

Muñoz-Sabater, J., Dutra, E., Agustí-Panareda, A., Albergel, C., Arduini, G., Balsamo, G., ... & Thépaut, J. N. (2021). ERA5-Land: A state-of-the-art global reanalysis dataset for land applications. *Earth system science data*, *13*(9), 4349-4383. https://doi.org/10.5194/essd-13-4349-2021

Mukherjee, S., & Mishra, A. K. (2021). Increase in compound drought and heatwaves in a warming world. *Geophysical Research Letters*, *48*(1), e2020GL090617. https://doi.org/10.1029/2020GL090617

Nouri, M. (2023). Drought assessment using gridded data sources in data-poor areas with different aridity conditions. *Water Resources Management*, *37*(11), 4327-4343. https://doi.org/10.1007/s11269-023-03555-4

Otón, G., Lizundia-Loiola, J., Pettinari, M. L., & Chuvieco, E. (2021). Development of a consistent global long-term burned area product (1982–2018) based on AVHRR-LTDR data. *International Journal of Applied Earth Observation and Geoinformation*, *103*, 102473. https://doi.org/10.1016/j.jag.2021.102473

Perkins-Kirkpatrick, S. E., & Gibson, P. B. (2017). Changes in regional heatwave characteristics as a function of increasing global temperature. *Scientific Reports*, *7*(1), 12256. https://doi.org/10.1038/s41598-017-12520-2

Perkins-Kirkpatrick, S. E., & Lewis, S. C. (2020). Increasing trends in regional heatwaves. *Nature communications*, *11*(1), 3357. https://doi.org/10.1038/s41467-020-16970-7

Petrou, I., & Kassomenos, P. (2025). Local factors contributing to daytime, nighttime, and compound heatwaves in the Eastern mediterranean. *Theoretical and Applied Climatology*, *156*(4), 194. https://doi.org/10.1007/s00704-025-05429-8

Rao, K., Williams, A. P., Diffenbaugh, N. S., Yebra, M., & Konings, A. G. (2022). Plant-water sensitivity regulates wildfire vulnerability. *Nature ecology & evolution*, *6*(3), 332-339. https://doi.org/10.1038/s41559-021-01654-2

Romanou, A., Hegerl, G. C., Seneviratne, S. I., Abis, B., Bastos, A., Conversi, A., ... & Suarez-Guiterrez, L. (2024). Extreme events contributing to tipping elements and tipping points. *Surveys in geophysics*, 1-46. https://doi.org/10.1007/s10712-024-09863-7

Runge, J. (2018). Causal network reconstruction from time series: From theoretical assumptions to practical estimation. *Chaos: An Interdisciplinary Journal of Nonlinear Science*, *28*(7). https://doi.org/10.1063/1.5025050

Runge, J., Nowack, P., Kretschmer, M., Flaxman, S., & Sejdinovic, D. (2019). Detecting and quantifying causal associations in large nonlinear time series datasets. *Science advances*, *5*(11), eaau4996. https://doi.org/10.1126/sciadv.aau4996

Runge, J., Gerhardus, A., Varando, G., Eyring, V., & Camps-Valls, G. (2023). Causal inference for time series. *Nature Reviews Earth & Environment*, *4*(7), 487-505. https://doi.org/10.1038/s43017-023-00431-y

Santos, R., Russo, A., & Gouveia, C. M. (2024). Co-occurrence of marine and atmospheric heatwaves with drought conditions and fire activity in the Mediterranean region. *Scientific Reports*, *14*(1), 19233. https://doi.org/10.1038/s41598-024-69691-y

Schreiber, T. (2000). Measuring information transfer. *Physical review letters*, *85*(2), 461. https://doi.org/10.1103/PhysRevLett.85.461

Sen, P. K. (1968). Estimates of the regression coefficient based on Kendall's tau. *Journal of the American statistical association*, *63*(324), 1379-1389. https://doi.org/10.1080/01621459.1968.10480934

Shan, B., De Baets, B., & Verhoest, N. E. (2024). Compound extreme climate events intensify yield anomalies of winter wheat in France. *Environmental Research Letters*, *19*(11), 114029. https://doi.org/10.1088/1748-9326/ad7ee6

Shi, Z., Jiang, D., & Wang, Y. (2024). Spatiotemporal dependence of compound drought–heatwave and fire activity in China. *Weather and Climate Extremes*, *45*, 100695. https://doi.org/10.1016/j.wace.2024.100695

Simanjuntak, C., Gaiser, T., Ahrends, H. E., Ceglar, A., Singh, M., Ewert, F., & Srivastava, A. K. (2023). Impact of climate extreme events and their causality on maize yield in South Africa. *Scientific Reports*, *13*(1), 12462. https://doi.org/10.1038/s41598-023-38921-0

Sutanto, S. J., Zarzoza Mora, S. B., Supit, I., & Wang, M. (2024). Compound and cascading droughts and heatwaves decrease maize yields by nearly half in Sinaloa, Mexico. *Npj Natural Hazards*, *1*(1), 26. https://doi.org/10.1038/s44304-024-00026-7

Sutanto, S. J., Duku, C., Gülveren, M., Dankers, R., & Paparrizos, S. (2025). Future intensification of compound and consecutive drought and heatwave risks in Europe. *Natural Hazards and Earth System Sciences*, *25*(10), 3879-3895. https://doi.org/10.5194/nhess-25-3879-2025

Tatli, H., & Serkendiz, H. (2025). Heatwave dynamics in Türkiye: a long-term spatiotemporal analysis of frequency, duration, and intensity (1970–2022). *Environmental Monitoring and Assessment*, *197*(7), 752. https://doi.org/10.1007/s10661-025-14246-5

Tian, R., Li, J., Zheng, J., Liu, L., Han, W., & Liu, Y. (2024a). The impact of compound drought and heatwave events from 1982 to 2022 on the phenology of Central Asian grasslands. *Journal of Environmental Management*, *365*, 121624. https://doi.org/10.1016/j.jenvman.2024.121624

Tian, Y., Giaquinto, D., Di Capua, G., Claassen, J. N., Ali, J., Li, H., & De Michele, C. (2024b). Historical changes in the Causal Effect Networks of compound hot and dry extremes in central Europe. *Communications Earth & Environment*, *5*(1), 764. https://doi.org/10.1038/s43247-024-01934-2

Tibau, X. A., Reimers, C., Gerhardus, A., Denzler, J., Eyring, V., & Runge, J. (2022). A spatiotemporal stochastic climate model for benchmarking causal discovery methods for teleconnections. *Environmental Data Science*, *1*, e12. https://doi.org/10.1017/eds.2022.11

Trenberth, K. E., Dai, A., Rasmussen, R. M., & Parsons, D. B. (2003). The changing character of precipitation. *Bulletin of the American Meteorological Society*, *84*(9), 1205-1218. https://doi.org/10.1175/BAMS-84-9-1205

Tripathy, K. P., Mukherjee, S., Mishra, A. K., Mann, M. E., & Williams, A. P. (2023). Climate change will accelerate the high-end risk of compound drought and heatwave events. *Proceedings of the National Academy of Sciences*, *120*(28), e2219825120. https://doi.org/10.1073/pnas.2219825120

Vicente-Serrano, S. M., Beguería, S., & López-Moreno, J. I. (2010). A multiscalar drought index sensitive to global warming: the standardized precipitation evapotranspiration index. *Journal of climate*, *23*(7), 1696-1718. https://doi.org/10.1175/2009JCLI2909.1

Wang, C., Li, Z., Chen, Y., Ouyang, L., Zhao, H., Zhu, J., ... & Zhao, Y. (2024). Characteristic changes in compound drought and heatwave events under climate change. *Atmospheric Research*, *305*, 107440. https://doi.org/10.1016/j.atmosres.2024.107440

Wang, C., Sun, X., Lu, N., & Qin, J. (2025). Impact of Rising Compound Drought and Heatwaves on Vegetation in Global Drylands. *IEEE Journal of Selected Topics in Applied Earth Observations and Remote Sensing, 18*, 24509 - 24517 https://doi.org/10.1109/JSTARS.2025.3610155

Westerling, A. L., Hidalgo, H. G., Cayan, D. R., & Swetnam, T. W. (2006). Warming and earlier spring increase western US forest wildfire activity. *science*, *313*(5789), 940-943. https://doi.org/10.1126/science.1128834

Yan, H., You, Y., Jiao, W., & Pan, N. (2025). Intensifying impacts of compound drought and heatwave events on water use efficiency in US corn and soybean. *Agricultural and Forest Meteorology*, *375*, 110873. https://doi.org/10.1016/j.agrformet.2025.110873

Yavaşlı, D. D., & Erlat, E. (2023). Climate model projections of aridity patterns in Türkiye: A comprehensive analysis using CMIP6 models and three aridity indices. *International Journal of Climatology*, *43*(13), 6207-6224. https://doi.org/10.1002/joc.8201

Yeşilköy, S., & Şaylan, L. (2022). Spatial and temporal drought projections of northwestern Turkey. *Theoretical and Applied Climatology*, *149*(1), 1-14. https://doi.org/10.1007/s00704-022-04029-0

Yeşilköy, S. (2025). Heatwave characteristics in agricultural and forest lands across Türkiye: Historical and future insights from CMIP6 simulations. *International Journal of Environment and Geoinformatics, 12*(4), 440-451. https://doi.org/10.26650/ijegeo.1701973

Yeşilköy, S., Baydaroğlu, O., Singh, N., Sermet, Y., & Demir, I. (2024). A contemporary systematic review of Cyberinfrastructure Systems and Applications for Flood and Drought Data Analytics and Communication. *Environmental Research Communications, 6,* 102003. https://doi.org/10.1088/2515-7620/ad85c4

Yeşilköy, S., & Demir, I. (2024). Crop yield prediction based on reanalysis and crop phenology data in the agroclimatic zones. *Theoretical and Applied Climatology*, *155*(7), 7035-7048. https://doi.org/10.1007/s00704-024-05046-x

Yeşilköy, S., & Baydaroğlu, Ö. (2025). Rain-on-snow climatology and its impact on flood risk in snow-dominated regions of Türkiye. *Theoretical and Applied Climatology*, *156*, 239. https://doi.org/10.1007/s00704-025-05463-6

Yeşilköy, S., Baydaroğlu, Ö., & Demir, I. (2026). Linking drought indicators and crop yields through causality and information transfer: a phenology-based analysis. *Scientific reports*. *16,* 2373. https://doi.org/10.1038/s41598-025-32185-6

Zhang, Q., She, D., Zhang, L., Wang, G., Chen, J., & Hao, Z. (2022). High sensitivity of compound drought and heatwave events to global warming in the future. *Earth's Future*, *10*(11), e2022EF002833. https://doi.org/10.1029/2022EF002833

Zhao, D., Zhang, Z., & Zhang, Y. (2023). Soil moisture dominates the forest productivity decline during the 2022 China compound drought-heatwave event. *Geophysical Research Letters*, *50*(17), e2023GL104539. https://doi.org/10.1029/2023GL104539

Zhu, X., Zhang, S., Zhang, Q., Lu, D., Tang, M., & Guo, C. (2025). Cascading impacts of compound drought-heat extremes on global gross primary production. *Climatic Change*, *178*(11), 207. https://doi.org/10.1007/s10584-025-04052-w

Zong, X., Yin, Y., & Yin, M. (2024). Climate change unevenly affects the dependence of multiple climate-related hazards in China. *npj Climate and Atmospheric Science*, *7*(1), 71. https://doi.org/10.1038/s41612-024-00614-4